D4.3 – Predictive control of the microgrid

Funded by the European Union. Views and opinions expressed are however those of the author(s) only and do not necessarily reflect those of the European Union or the European Commission. Neither the European Union nor the granting authority can be held responsible for them.

Deliverable 4.3 – Predictive control of the microgrid

TwInSolar

(Improving Research and Innovation to achieve a massive integration of Solar renewables)

Organisation: laboratory PIMENT

Main author: Mathieu DAVID (UR)

Contributors: Faly RAMAHATANA (UR), Josselin LE GAL LA SALLE (UR), Philippe LAURET (UR), Elke LORENZ (Fraunhofer ISE)

This document has been developed as part of the project titled "**TwInSolar – Improving research and innovation to achieve a massive integration of solar renewables**"

The TwInSolar project (September 2022 - August 2025) has received funding from the European Union's Horizon Europe research and innovation programme under grant agreement No. 10107647

Document information

Deliverable:	D 4.3
Work Package:	WP4 – A smart solar microgrid in a tropical island
Task:	T4.3 – Smart management with forecast
Author:	Mathieu David
Document type:	Report
Dissemination level:	Public
Copyright:	Copyright © 2025, TwInSolar Consortium – All right reserved

Revision

Version	Date	Author	Description of changes
V1	02-11-2025	Mathieu David	First draft
V2	14-11-2025	Elke Lorenz	Review
V3	20-11-2025	Mathieu David	Final corrections and layout

Contents

Executive summary

The deliverable details the strategy proposed to manage the Terre Sainte campus microgrid. Based on a predictive EMS, that used solar forecast as input, the management aims at minimizing the operating cost of the microgrid. Results of other tasks of TwInSolar supported the development the predictive EMS. To design and size the microgrids components, we used ERMESS, which is a numerical tool presented in the deliverable D4.2 Microgrid design. We used the methods presented during the summer school of WP3, to generate the different solar forecasts. Finally, the content of this deliverable was presented at the ISES Solar World Congress that took place in Fortaleza, Brazil, 4th-7th November 2025.

Energy Management Systems (EMS) are essential for the optimal operation of energy systems powered by solar renewables like photovoltaics (PV). They increase local renewable energy use while ensuring affordable energy prices for end users. Predictive EMS, based on solar forecasts, promise to be more efficient than ruled-based EMS commonly implemented in operational systems such as microgrids. However, the selection and integration of the most relevant solar forecasts in the optimization process of EMS are rarely addressed in the literature. This work proposes to compare different EMS and state-of-the-art solar forecasts in order to minimize the operating cost of a campus microgrid.

In the case study considered, the predictive EMS achieves a microgrid operating cost 10% lower than that of a standard rule-based EMS. The higher the quality of the forecasts used as input of the predictive EMS, the lower the operating cost. However, with a microgrid self-sufficiency of 84%, the rule-based EMS offers a good compromise between technical and economic performance. These results will provide useful information to microgrid managers for the development and operation of their systems.

I. Introduction

Future energy systems will rely significantly on solar renewables, a mature and cost-effective solution. However, the variability of solar production requires increased flexibility in energy systems to compensate for these fluctuations. Microgrid and building energy systems can provide the desired flexibility. In this context, energy management systems (EMS) play a key role in exploiting this flexibility while maintaining affordable energy cost. Among the wide variety of management techniques dedicated to microgrid operation, predictive EMS based on production and load forecasts seem to be more efficient (Mazzola et al., 2017). However, most of the works on predictive EMS use perfect foreseen or simplified forecast methods (Le Franc et al., 2023). In this work we will focus on the use of state-of-the-art solar forecasts to minimize the operating cost of a microgrid.

In the past years, numerous techniques have been proposed to generate short-term forecasts of solar irradiance and corresponding photovoltaic (PV) production (Lorenz et al., 2024). These methods were developed to meet specific needs. They therefore cover various time horizons and spatial areas. For example, intra-hourly forecasts based on time series models are suitable for single-site and real-time management, while day-ahead forecasts based on numerical weather prediction (NWP) can cover a region and are relevant for planning unit commitment and energy dispatching (Antonanzas et al., 2016; Diagne et al., 2013). Moreover, forecast can be deterministic or probabilistic. Among all these possibilities, the choice of the most valuable forecast is not straightforward.

To make the optimal decision, predictive management of a microgrid requires simultaneously anticipating the fluctuations that will occur in the coming minutes and the energy balance between production and load over a longer time horizon. Therefore, we assume in this work that a specific technique, which covers a limited range of forecast horizons, is not suitable as input to a predictive EMS. The use of blending of forecasts from different methods, such as NWP, Cloud Motion Vectors (CMV) applied to satellite images (Lorenz et al., 2016; Straub et al., 2024) and time series models, which spans horizons from a minute to several days ahead, should solve this issue.

In this work we propose to compare the economic performance of different EMS and solar forecasts to minimize the operating cost of a university campus microgrid. Load forecasting is not taken into account and we will assume perfect knowledge of the future consumption of the microgrid. The contribution of this work is twofold. First, a method for integrating forecasts into the optimization process of a predictive EMS is detailed and compared with that of a conventional rule-based (RB) EMS (Lambert et al., 2005). Then, to help microgrid managers choose the most relevant solar forecast, we compare the economic performance of state-of-the-art techniques, ranging from a naive forecast (i.e., persistence) to an advanced forecast based on a combination of NWP, satellite, and time-series.

The structure of the paper is as follows. The next section presents the case study, a university campus microgrid, used to compare different solar forecasts and EMS. The methods used to generate the deterministic and probabilistic PV production forecasts are detailed in Section 3. Section 4 provides an overview of the two types of EMS compared in this work. The results are then presented and analyzed in Section 5 before concluding.

II. Case study

The university campus considered in this work is located in the city of Saint-Pierre, La Reunion, which is a tropical island in the southern part of the Indian Ocean. The campus hosts approximately 1,500 students for a total floor area of 19,000 m^2. The campus has a student residence, a restaurant and classical university buildings. The campus consumes 1,185 GWh of electricity annually. It already has 167 kW of PV installed on its roofs and an extension of the PV capacity is planned (Randrianantenaina et al., 2025). The microgrid, which does not include an energy storage system (ESS), has a self-sufficiency of around 16%. It is fully monitored. A set of publicly available data with a time step of 10 minutes and for two consecutive years (2021 and 2022) provides weather variables, advanced solar irradiance data, PV productions and electrical loads for each building (David et al., 2023).

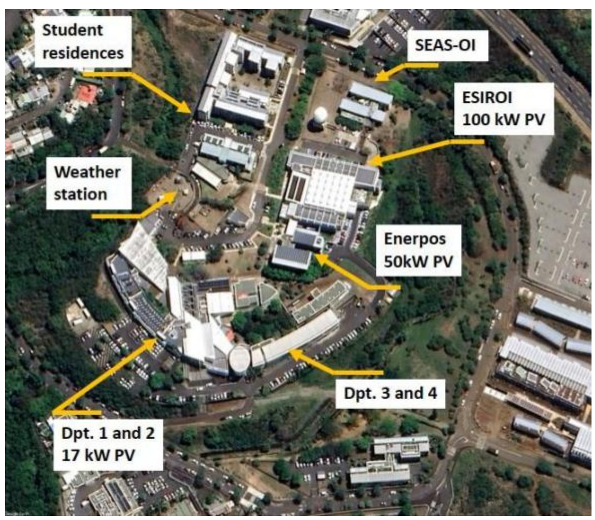

Fig. 1: Overview of the university campus located in the city of Saint-Pierre, La Reunion

To study the performances of different EMS and solar forecasts, we use a microgrid design that permits to reach 80% self-sufficiency with a cost of energy slightly above the current average electricity price of approximately 0.18€/kWh. Based on the data collected on the actual system, we used the ERMESS tool to design and size the microgrid's components (Le Gal La Salle et al., 2024). The optimization resulted in a PV capacity multiplied by 4 and distributed on the existing roofs of the campus, and Li-ion batteries with an energy capacity of 1,548 kWh. Table 1 details the sizing of the microgrid and associated cost.

Among the different electricity purchase prices proposed by the distribution system operator, ERMESS also select the most advantageous one. In our case, the best tariff differs depending on the hour of the day and the season. The electricity purchase price (C_{grid}) oscillates between 0.116€/kWh during off-peak hours of the low season (April to October) to 0.35€/kWh for peak hours (from 6pm to 10pm) in high season. For a detailed description of the prices the reader is referred to the "Transition énergétique" tariff of EDF Réunion (EDF Réunion, 2022). The PV installation is dedicated to increase the self-sufficiency of the microgrid. Therefore, no feed-in tariff is envisaged and the export of energy to the grid is not permitted. We computed the levelized cost of storage and levelized cost of PV production using the methodology proposed by (Short et al., 2005) and (Pawel, 2014). However, in this work, we used extremely simplified assumptions. For example, we did not retain any discount rate. ERMESS estimated the PV production and the energy transferred to the ESS only for the test period and optimal energy management. Therefore, we extrapolated the annual energy quantities. In further research, these economic indicators should be evaluated using a more advanced approach.

Table 1: Microgrid optimal sizing obtained with the ERMESS tool for 80% self-sufficiency

Parameter	Symbol	Value
Total installed PV power	P_{pv}	692.8 kW
ESS capacity	ESS_{capa}	1,548 kWh
Maximum charging / discharging power	P_{ess}^{cha} / P_{ess}^{dis}	217 kW / 217 kW
State of charge (SOC) min / max	SOC_{min} / SOC_{max}	10% - 100%
ESS and converter round trip efficiency	η_{ess}	80%
Levelized cost of storage	C_{ess}	0.16 €/kWh
Levelized cost of PV production	C_{pv}	0.06 €/kWh

II. Solar forecasts

To compare the performance of predictive EMS with different forecasting techniques as input, we generated a set of four PV production forecasts spanning from a naïve and simple deterministic model to the most advanced probabilistic model derived from a blending of multiple prediction sources. The first step of our generation process is the deterministic forecasting of the future available global horizontal solar irradiance (GHI). Then we estimate the future PV production from the GHI forecast. And finally, we post-process the deterministic PV production forecast to obtain a probabilistic prediction. To be consistent with the available monitoring data and the required level of anticipation of the EMS, the generated forecasts have a time resolution of 10 minutes and covers horizons up to 2 days ahead. Therefore, every 10-min time step of the considered period, a new forecast is issued for the next 48 hours with a 10-min granularity. The different sources of forecast are available for a period of 6 months, from July 1st to December 31st, 2022. To create the final PV production forecasts, we divided the dataset into a training and test period covering respectively the first 70% part of the period (from July 1st to November 11th) and the last 30% of the period (from November 12th to December 31st). The initial GHI forecasts used in this work are publicly available on a GitHub repository prepared for a summer school organized during the project TwInSolar (David et al., 2024).

A) GHI deterministic forecasts

Among the numerous solar irradiance forecasting techniques of the literature, we selected the relevant ones for three distinct time horizons: the smart persistence for intra-hour, satellite-based forecast for intra-day (from 30 minutes to 6 hours ahead) and NWP for day-ahead (from 6 hours to 48 hours ahead) (Antonanzas et al., 2016; Diagne et al., 2013). The smart persistence of the clear-sky index is a naive model based only on historical values of GHI. Even if the persistence performs better for very short-term horizons, to use it with the predictive EMS, we generated GHI predictions for the next 2 days as follow:

$$\widehat{GHI}_{Persistence}(t+h) = \frac{\sum_{i=0}^{N_h} kt^*(t-i)}{N_h} GHI_{csk}(t+h). \qquad \text{(eq. 1)}$$

In equation 1, GHI_{csk} is the global horizontal irradiance under clear sky conditions. For this work, we used the clear sky data from the McClear model (Lefèvre et al., 2013). kt^* is the clear sky index corresponding to the observed GHI divided by the clear sky GHI. N_h is the number of time steps between the current time t and the considered horizon h.

The second technique used sequences of images from the stationary meteorological satellite MSG-IODC to extrapolate the future position of the clouds and then to derive the future solar irradiance. The method estimates cloud motion vectors (CMV) that describe cloud movement as a 2D vector field (Lorenz et al., 2024). Satellite forecast performs best for horizons ranging from 30 minutes to 4-6 hours. The satellite forecasts generated for the considered location and period have a horizon of up to 6 hours ahead with a 30-min resolution. Consequently, the satellite forecast has only been used to create a blend of the three forecasting techniques. The third technique is the NWP, which is more relevant for forecasting horizons above 6 hours ahead. For this work we used the high-resolution deterministic forecast of the Integrating Forecasting System (IFS) provided by the European Centre of Medium range Weather Forecast (ECMWF) (Owens & Hewson, 2018). We used the forecast generated at 00:00 UTC and 12:00 UTC, with a 2-day horizon, a 1-hour resolution, and the closest pixel to the considered location. As the time resolution of the 3 sources of forecast differs, we aligned the data to be consistent with the observed PV production and load, which have a 10-min granularity. We applied the oversampling method proposed in the project ENDORSE (Espinar et al., 2011) to increase the time resolution of the NWP and satellite forecasts.

To obtain a forecast with good performance over all horizons necessary for the optimal management of the microgrid, we blended the three forecast sources with a linear approach (Lorenz et al., 2016) as follow:

$$\widehat{GHI}_{Blend}(t+h) = a_h \times \widehat{GHI}_{Persistence}(t+h) + b_h \times \widehat{GHI}_{Satellite}(t+h) + c_h \times \widehat{GHI}_{NWP}(t+h). \quad \text{(eq. 2)}$$

In equation 2, the coefficients a_h, b_h and c_h, which depend on the horizon h, are estimated by the ordinary least square method. Since satellite forecasts are not available for horizons above 6 hours, we combined the three sources only for the first 6 hours. For horizons longer than 6 hours, the combined GHI corresponds to the NWP. This choice is supported by the forecast quality assessment presented in Figure 4 of section 5. To conclude, we have three GHI forecasts that can be used for the following steps: the persistence ($\widehat{GHI}_{Persistence}$), the NWP ($\widehat{GHI}_{NWP}$) and the blend ($\widehat{GHI}_{Blend}$).

B) PV production deterministic forecasts

From the three GHI forecasts, we derived three deterministic PV production forecast using a classical PV plant modelling approach. First, we divided the GHI into direct and diffuse irradiance with the BRL decomposition model (Ridley et al., 2010). Second, we estimated the plane of array irradiance of each roof using the Perez transposition model (Perez et al., 1990). Then, we computed the back temperature of panels using the Sandia Photovoltaic Array Performance Model (SAPM) (King et al., 2004). And finally, we obtained the PV plant production using the simple and efficient PVWATT methods (Dobos, 2014). To automate the conversion from GHI to PV production, we used the Python library pvlib (F. Holmgren et al., 2018), that have all the models presented above. Figure 2 shows an example of the three PV production deterministic forecasts, with a horizon of 1 hour, and corresponding observations.

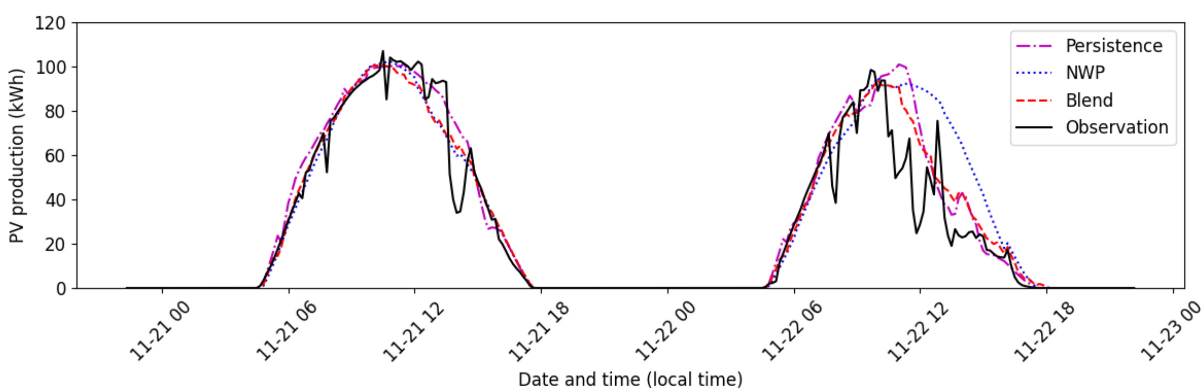

Fig. 2: Two days of deterministic PV production forecasts from 3 different techniques (persistence, NWP and blend) with a horizon of 1 hour

C) PV production probabilistic forecast

To create a PV production probabilistic forecast, we post-processed the blended deterministic forecast as proposed by Lauret et al. (Lauret et al., 2024). We only considered the deterministic forecast of PV production as a single input to a machine learning process, here a Gradient Boosting Decision Trees (GBDT), to generate a set of 11 quantiles (0.01, 0.1, 0.2, …, 0.99). Figures 3 illustrates 2 days of probabilistic forecast with a horizon of 1 hour and the prediction intervals resulting from the generated quantiles.

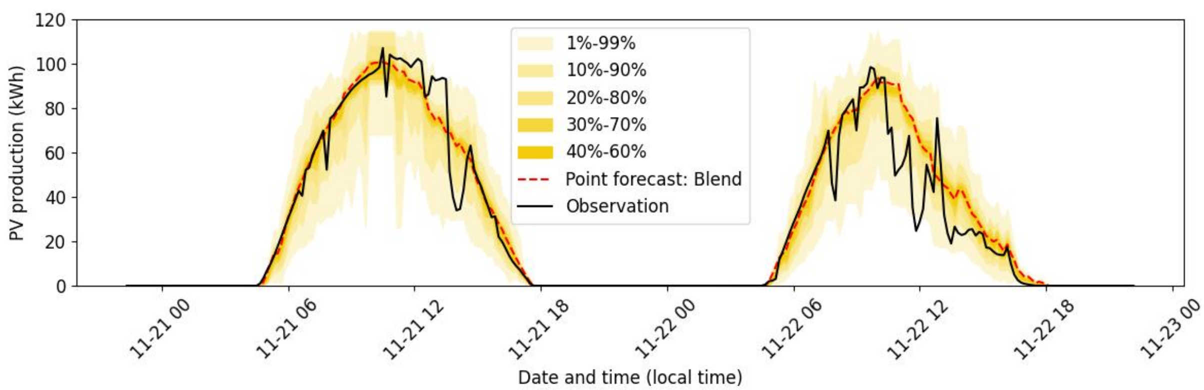

Fig. 3: Two days of deterministic PV production forecasts (blend) and the corresponding probabilistic forecasts derived with the GBDT model (prediction intervals in yellow) with a horizon of 1 hour

D) Evaluation of forecast quality

The quality of a forecast measures the deviation between a prediction and the corresponding outcome. Relevant methodologies and metrics are proposed to evaluate of the quality of solar deterministic (Yang et al., 2020) and probabilistic forecasts (Lauret et al., 2019). In this work, for sake of simplicity, we restricted our evaluation to error metrics widely used by the solar forecasting community. The Mean Bias Error (MBE), the Root Mean Square Error (RMSE) and the Mean Absolute Error (MAE) quantify the quality of deterministic forecasts. The Continuous Rank Probability Score (CRPS) measures the quality of probabilistic forecasts. The latter corresponds to the MAE for a deterministic forecast, thus allowing the direct comparison of the quality of deterministic and probabilistic forecasts. The following four equations give the formulas of the four metrics presented above:

$$MBE = \frac{1}{N}\sum_{i=1}^{N}(\widehat{y_i} - y_i), \qquad \text{(eq. 3)}$$

$$RMSE = \sqrt{\frac{1}{N}\sum_{i=1}^{N}(\widehat{y_i} - y_i)^2}, \qquad \text{(eq. 4)}$$

$$MAE = \frac{1}{N}\sum_{i=1}^{N}|\widehat{y_i} - y_i|, \qquad \text{(eq. 5)}$$

$$CRPS = \frac{1}{N}\sum_{i=1}^{N}\int_{-\infty}^{+\infty}\left[\widehat{F_i}(x) - (x)\right]^2 dx. \qquad \text{(eq. 6)}$$

In the equations 3 to 6, y_i and $\widehat{y_i}$ are respectively the observed PV production and the corresponding forecast. N is the number of forecast/observation pairs used to compute the error metrics. In equation 6, F_i and $\widehat{F_i}$ are the observed and forecast cumulative distribution functions (CDF) of the GHI. As the errors of forecast are null during the night, we compute the error metrics considering only daytime, when the observed PV production is greater than 0 ($y > 0$). Finally, to have a fair comparison of the different forecasting horizons, we normalize the error metrics by the average observed PV production $\frac{1}{N}\sum_{i=1}^{N} y_i$.

III. Energy Management System (EMS)

A) Predictive EMS

The objective of the predictive EMS system is to minimize the microgrid operating cost, which is a linear combination of grid electricity purchases, renewable energy generation cost, and ESS operating cost. The main decision variables are the ESS charging and discharging energy (E_{ess}^{cha} and E_{ess}^{dis}), the photovoltaic generation (E_{pv}), and the energy purchased from the grid (E_{grid}). In our case study, we do not consider any controllable loads. Therefore, the EMS cannot provide demand management. The optimization is subject to classical energy system constraints, such as ESS capacity, maximum converter power, and overall energy balance. To simplify the problem and solve it by linear programming, we assume constant converter efficiency. The mathematical formulation of the optimization problem is:

Objective function:

$$min_{\{E_{ess}^{dis}, E_{ess}^{cha}, E_{pv}, E_{grid}\}} = \sum_{t=1}^{N} E_{grid}(t) \cdot C_{grid}(t) + E_{ess}^{dis}(t) \cdot C_{ess} + E_{pv}(t) \cdot C_{pv}, \qquad \text{(eq. 7)}$$

where N is the number of considered time steps. As we optimize the operation of the microgrid for the next 2 days with a 10-min resolution, $N = 288$.

Subject to:

Energy balance: $E_{grid}(t) + E_{pv}(t) - E_{load}(t) + E_{ess}^{dis}(t) - E_{ess}^{cha}(t) = 0,$ (eq. 8)

SOC evolution: $[SOC(t) - SOC(t-1)] \cdot ESS_{capa} = E_{ess}^{cha}(t-1) \cdot \sqrt{\eta_{ess}} - \frac{E_{ess}^{dis}(t-1)}{\sqrt{\eta_{ess}}},$ (eq. 9)

Power limitations: $\begin{matrix} 0 \le E_{ess}^{cha}(t) \le P_{ess}^{cha} \cdot dt \\ 0 \le E_{ess}^{dis}(t) \le P_{ess}^{dis} \cdot dt \end{matrix},$ (eq. 10)

SOC limitations: $SOC_{min} \le SOC(t) \le SOC_{max}$, (eq. 11)

Maximum possible PV production: $E_{pv}(t) \le \hat{E}_{pv}(t)$. (eq. 12)

In equation 12, we introduce the PV production forecast $\hat{E}_{pv}(t)$ as the upper limit of the PV production. As the export to the grid is not possible, the EMS can curtail the PV production to ensure the energy balance within the microgrid (equation 8). To anticipate future variations of the PV production beyond the next step, we used a receding horizon approach to integrate the forecast in the optimization problem. We solve the optimization at each time step with an updated forecast with a time horizon of 48 hours and use only the decision of the next step.

Therefore, the optimization provides the optimal decisions for the next 48 hours, but the EMS applies only the decision taken for the next time step.

With the deterministic PV production forecast, we solved the optimization problem with the Ipopt solver of the Python library Pyomo, which is a classical Mixed Integer Linear Programming solver. For the probabilistic forecast, we used a solver based on the Probabilistic Dynamic Programming (PDP) method and specifically designed for microgrid EMS (Ramahatana et al., 2022). The objective function is slightly different from the deterministic approach given by equation 7. Instead of minimizing operating cost, the PDP minimizes the expectancy of the operating cost over all quantiles of the probabilistic forecast. Due to the very high computational time of the probabilistic solver, we decided to limit the frequency of optimizations. Thus, for probabilistic forecasts, we solved the optimization problem only once a day, compared to every 10 minutes for the deterministic approach.

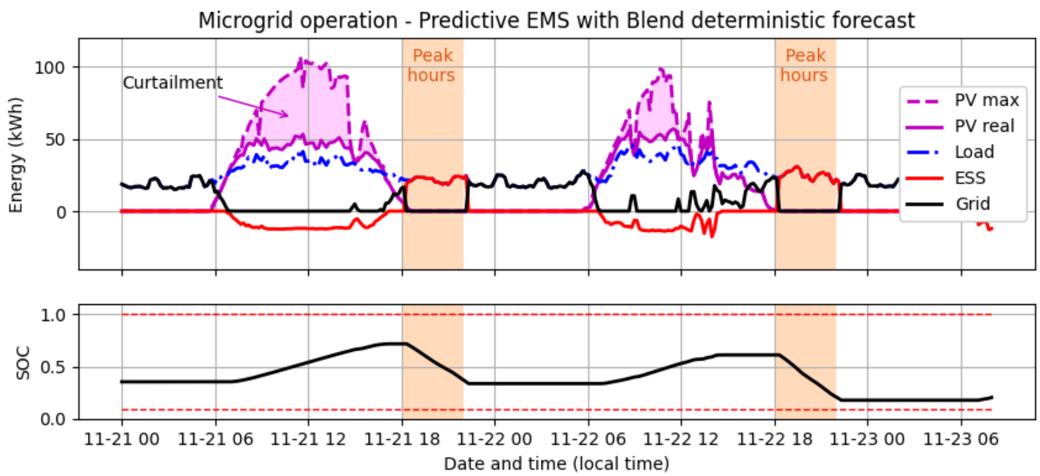

Fig. 4: Two days of operation of the microgrid with predictive EMS and the "Blend" deterministic PV production forecast (upper plot) and corresponding ESS state of charge (lower plot)

Because forecasts are inherently uncertain, actual PV production differs from forecast. To compensate for these discrepancies, we have implemented real-time management, similar to a Power Management System (PMS). This system cannot modify the operation of the ESS planned by the EMS. It is only authorized to update the amount of energy imported from the grid to compensate for lower than forecast PV production. Figure 4 shows an example of two days of microgrid operation with the blended deterministic forecast as input to the EMS. During daytime, the EMS decides to supply the load and charge the ESS with PV production. The difference between available PV production (dashed magenta line) and actual PV production (solid magenta line), highlighted by a light magenta area, indicates a reduction. The small peaks of grid energy import (plain black line) that occur during daytime are due to errors of forecast. The plain red line plots the ESS charge (negative) and discharge (positive). During the evening peak hours (6 p.m. – 10 p.m.), when the electricity price is high, the EMS orders to supply the load with the ESS.

We see that the EMS anticipates lower PV production on the second day, because it decides not to fully discharge the ESS during the night.

B) Reference rule-based EMS

To assess the efficiency of the solar forecast based predictive EMS, we compared it to a well-known ruled-based EMS named Load Following (LF), which is detailed in the documentation of the software HOMER (Lambert et al., 2005). This reference rule-based EMS is actually used by most of the residential hybrid power plants. Simple rules define a priority ranking among the available energy sources to supply the load. In our case, the priority order is: first the PV production, then the ESS discharge and finally the main grid. When PV production is higher than load, the excess energy charges the ESS. And when the storage is full, the excess energy is curtailed or feed-in to the grid. In our case, as we do not consider any feed-in tariff, both actions result in an identical economic value with no gain.

Figure 5 shows an example of microgrid operation with the rule-based EMS for the same days as in Figure 4. Due to the converter power limit, we observe a slight PV production curtailment on the first day. The rule-based strategy tends to fully charge and discharge the ESS each day. Because it does not anticipate the drop in PV production on the second day, the system is empty before peak demand. As a result, the microgrid must purchase electricity at a high price between 6 p.m. and 10 p.m. on the second day.

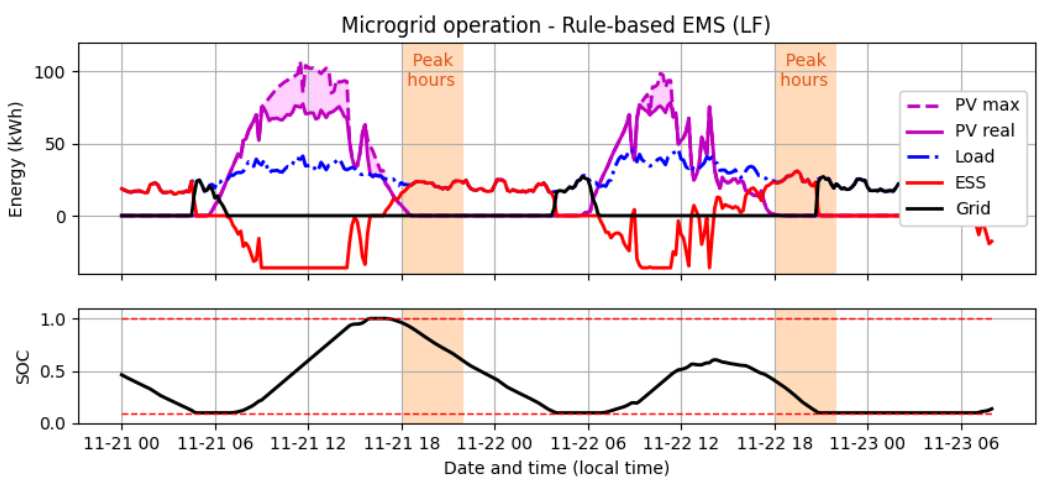

Fig. 5: Two days of operation of the microgrid with rule-based EMS (upper plot) and corresponding ESS state of charge (lower plot)

IV. Results and discussions

The quality of the generated solar forecasts and the performances of the different EMS are evaluated on 49 days of the test period, from November 12th to December 31st, 2022. Therefore, in this section, all the indicators are derived from results obtained during this period. First, we will evaluate the quality of the different PV production forecast and then we will assess the performance of the different EMS.

A) Evaluation of the quality of the PV production forecasts

Figure 4 presents the error metrics defined in Section 3.4 for the four PV production forecasts. It shows the results for horizons ranging from 30 minutes to 12 hours. Beyond 12 hours, the value of the error metrics remains almost constant. For readability, we have chosen not to graphically represent the entire 72-hour horizon. For the shortest forecast horizons, less than 1 hour, persistence has lower RMSE and MAE than NWP. However, for longer horizons, NWP outperforms persistence. At a 6-hour horizon, we can see a jump in the MBE and MAE of the blended deterministic forecast (dashed red line). This jump corresponds to the junction between the horizons where the blending of forecast sources is actually achieved (i.e. from 10 minutes to 6 hours) and the horizons beyond which the blended deterministic forecast is equal to the NWP. Therefore, it cannot be considered as perfectly seamless. As expected, the blended deterministic forecast exhibits better RMSE for all time horizons. Moreover, the jump is not visible for the RMSE curve. Both observations result from the method used to calculate the coefficients of the linear combination of forecasting sources, which minimizes the square error.

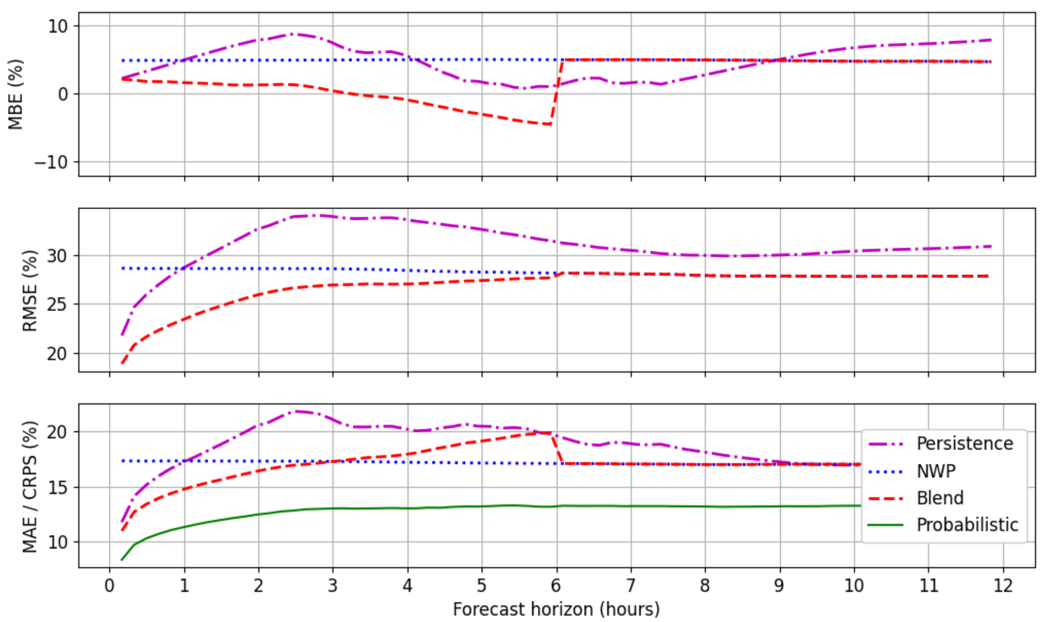

Fig. 6: Evaluation of the quality of the deterministic and probabilistic forecasts with three error metrics (MBE, MAE/CRPS and RMS for the testing period

In summary, persistence provides good quality for forecast horizons shorter than one hour. Numerical weather prediction (NWP) outperforms persistence for longer horizons. Moreover, among the three deterministic forecasts considered in this work, the blended forecast has the best quality for all horizons. Therefore, testing these three forecasts as input data for the predictive EMS allows estimating the most significant horizons to optimize microgrid operation.

The probabilistic prediction (plain green line), which is derived from the blended deterministic forecast, has a better quality, measured by the CRPS, than the deterministic forecasts. We can reasonably assume that the postprocessing of the blended deterministic forecast and the estimation of the quantiles, that is a quantification of the uncertainty associated to the prediction, significantly improve the quality. We will see, in the next subsection, if this improvement will result in a better value for the users.

B) EMS performances

In this work, we evaluate the economic and technical performances of the different EMS, which can be considered as a quantification of the value for microgrid users. Economic efficiency is the operating cost given by equation 7, divided by the total load. Expressed in euros per kilowatt-hour, this value is equivalent to the well-known levelized cost of energy (LCOE) from the end user's perspective. Lower is the operating cost, better the economic efficiency of the microgrid. The self-sufficiency evaluates the technical performance of the microgrid and, in some extent, its carbon emission. The self-sufficiency is the share of the load supplied by the onsite energy generation. Table 2 summarizes performances of the different EMS.

Table 2: Economical and technical performances of the different EMS and forecasts

EMS	Operating cost	Self-sufficiency
Rule-based (LF)	0.1381 €/kWh	89.7%
Predictive with Persistence forecast	0.1208 €/kWh	62.32%
Predictive with NWP forecast	0.1198 €/kWh	63.2%
Predictive with Blend forecast	0.1193 €/kWh	63.8%
Predictive with probabilistic forecast	0.1286 €/kWh	67.3%
Predictive EMS with perfect forecast	0.1176 €/kWh	65.3%
Without PV, ESS and EMS	0.1897 €/kWh	0%

To better assess the economic value of the microgrid combined with an EMS, the last rows of Table 2 provide two benchmarks. First, the campus without PV, ESS, or EMS quantifies the worst-case scenario. It corresponds to 100% of the load being supplied by the grid. Second, the predictive EMS, with perfect PV production forecasts as input, offers the lowest possible operating cost. These two scenarios indicate the lower and upper limits of the microgrid operating cost. Interestingly, the creation of a microgrid for the Terre Sainte campus saves up to 37% of operating costs, which corresponds to a potential annual saving of around 80,000 €.

The operating cost of the rules-based EMS is higher than that of the different versions of the predictive EMS, regardless of the forecast used. Overall, the predictive approach reduces the operating cost by approximately 11%-15% compared to the rule-based EMS. Focusing on predictive EMS, the differences in economic value between the three deterministic forecasts are relatively small, less than 1.5%. Using NWP results in slightly lower operating costs than using persistent forecasts. The use of the blended deterministic forecasting further reduced operating costs. However, the difference between the NWP and the blended forecast, 0.0005 €/kWh, is negligible. This result tends to demonstrate that longer horizons of forecast bring more value than shorter ones. With probabilistic forecasts, even if the decision-making is only once a day, predictive EMS achieves an operating cost close to that obtained with deterministic forecasts. With a higher frequency, the results of the probabilistic predictive EMS should be very close to the perfect forecast. However, computation time remains a major obstacle to its use in an operational system.

With a self-sufficiency of 84.6% over the period considered, the rule-based EMS performs significantly better than the predictive approach. Indeed, the latter leads to a self-sufficiency slightly above 60%. Since the objective of the predictive EMS is to minimize the operating cost of the microgrid, the self-sufficiency rate is a consequence of its decisions. It is worth noting that better forecast quality allows for greater self-sufficiency and simultaneously a reduction in operating costs. However, the initial goal of the microgrid is to achieve 80% self-sufficiency at an affordable energy cost. Although the predictive EMS offers the lowest energy cost, it does not guarantee the desired level of self-sufficiency. Thus, compared to a predictive EMS exclusively dedicated to minimizing operating costs, the rule-based EMS seems to provide a good compromise between economic and technical performance.

The results of this study should be interpreted with caution. They obviously depend on the case study used to illustrate them. Moreover, we used a very simplified calculation of the energy storage cost and the PV production cost (see Table 1) using the output of the ERMESS tool. For instance, to calculate the PV production cost, we extrapolated the annual PV production from a reduced set of days covering less than two months. In addition, with the ERMESS tool, we assumed perfect energy management optimizing operating costs while respecting a self-sufficiency constraint of 80%. Such a management strategy, which implies perfect knowledge of PV production and load for the entire considered period, is not possible in real operation. Consequently, the total PV production and energy transfer via storage, used during sizing step, could be significantly different from the quantities resulting from the actual operation of the EMS. Ideally, the actual EMS operation should be considered at the sizing stage.

V. Conclusion and perspectives

In this work, we evaluated the economic and technical performances of a predictive EMS used for the operation of a university campus microgrid powered by rooftop PV systems and the electrical grid. As input to the EMS, we generated PV production forecasts of increasing quality:

from naive deterministic persistence to the most advanced probabilistic prediction, based on a combination of different forecast sources. We compared the performance of the predictive approach to that of a rule-based EMS, commonly used for the operation of residential microgrids.

As the objective of the predictive EMS is to minimize the operating costs of the microgrid, it logically outperforms the economic performance of the rule-based EMS, thus enabling microgrid users to obtain the lowest energy cost. The results show that a better quality of the forecast improves simultaneously the operating cost and the self-sufficiency of the microgrid. Moreover, it appears that high quality of longer forecast horizons adds more value. However, the rule-based EMS results in a significantly better self-sufficiency of the microgrid and offers a good trade-off between economic efficiency and technical efficiency.

This work is a first attempt to comparatively evaluate the performance of different types of energy management systems (i.e., rule-based and predictive) and the added value of using forecasts of increasing quality for the operation of a university campus microgrid. A predictive energy management system solely dedicated to minimizing operating costs cannot also achieve environmental objectives. The proposed EMS needs to be further improved to also improve the environmental performance of the microgrid. For example, we could add constraints on self-sufficiency.

The PV production cost and the operating cost of the ESS used in the objective function of the predictive EMS are derived from the microgrid design and sizing tool ERMESS. However, the latter assumes perfect knowledge of the PV production and load over the entire period to manage the microgrid energy transfers. Therefore, the implementation of a real EMS operation at the microgrid sizing stage is necessary to better evaluate its performance and its impact on the sizing of the microgrid components.

References

Antonanzas, J., Osorio, N., Escobar, R., Urraca, R., Martinez-de-Pison, F. J., & Antonanzas-Torres, F. (2016). Review of photovoltaic power forecasting. Solar Energy, 136, 78–111. https://doi.org/10.1016/j.solener.2016.06.069

David, M., Grimes, W., Straub, N., Trovalet, L., & Voivret, C. (2024). TwInSolar summer school data [Csv, NetCDF]. GitHub. https://github.com/Laboratoire-Piment/TwInSolar-Summer_shool_data/

David, M., Le Gal La Salle, J., Vigneron, J., Trovalet, L., & Randrianantenaina, T. A. (2023). A set of consolidated data for the microgrid of Terre Sainte campus [Csv]. GitHub. https://github.com/Laboratoire-Piment/TwInSolar_consolidated_data

Diagne, M., David, M., Lauret, P., Boland, J., & Schmutz, N. (2013). Review of solar irradiance forecasting methods and a proposition for small-scale insular grids. Renewable and Sustainable Energy Reviews, 27, 65–76. https://doi.org/10.1016/j.rser.2013.06.042

Dobos, A. (2014). PVWatts Version 5 Manual (No. NREL/TP-6A20-62641, 1158421; p. NREL/TP-6A20-62641, 1158421). https://doi.org/10.2172/1158421

EDF Réunion. (2022, August 1). Grille de prix, tarif vert. EDF. https://reunion.edf.fr/sites/sei_reu/files/2022-04/vert-entreprise-reunion.pdf

Espinar, B., Wald, L., Blanc, P., Hoyer-Klick, C., & Schroedter-Homscheidt, M. (2011). Report on the harmonization and qualification of meteorological data, Project ENDORSE.

F. Holmgren, W., W. Hansen, C., & A. Mikofski, M. (2018). pvlib python: A python package for modeling solar energy systems. Journal of Open Source Software, 3(29), 884. https://doi.org/10.21105/joss.00884

King, D. L., Boyson, W. E., & Kratochvil, J. A. (2004). Photovoltaic Array Performance Model (Nos. SAND2004-3535). Sandia National Laboratories.

Lambert, T., Gilman, P., & Lilienthal, P. (2005). Micropower System Modeling with Homer. In F. A. Farret & M. G. Simões (Eds.), Integration of Alternative Sources of Energy (1st ed., pp. 379–418). Wiley. https://doi.org/10.1002/0471755621.ch15

Lauret, P., Alonso-Suárez, R., Amaro E Silva, R., Boland, J., David, M., Herzberg, W., Le Gall La Salle, J., Lorenz, E., Visser, L., Van Sark, W., & Zech, T. (2024). The added value of combining solar irradiance data and forecasts: A probabilistic benchmarking exercise. Renewable Energy, 237, 121574. https://doi.org/10.1016/j.renene.2024.121574

Lauret, P., David, M., & Pinson, P. (2019). Verification of solar irradiance probabilistic forecasts. Solar Energy, 194, 254–271. https://doi.org/10.1016/j.solener.2019.10.041

Le Franc, A., Carpentier, P., Chancelier, J.-P., & De Lara, M. (2023). EMSx: A numerical benchmark for energy management systems. Energy Systems, 14(3), 817–843. https://doi.org/10.1007/s12667-020-00417-5

Le Gal La Salle, J., David, M., & Lauret, P. (2024, September 23). Finding the optimal size and design of microgrid energy systems using a genetic algorithm. EU PVSEC 2024, 41st European Photovoltaic Solar Energy Conference and Exhibition, Vienne, Austria.

Lefèvre, M., Oumbe, A., Blanc, P., Espinar, B., Gschwind, B., Qu, Z., Wald, L., Schroedter-Homscheidt, M., Hoyer-Klick, C., Arola, A., Benedetti, A., Kaiser, J. W., & Morcrette, J.-J. (2013). McClear: A new model estimating downwelling solar radiation at ground level in clear-sky conditions. Atmospheric Measurement Techniques, 6(9), 2403–2418. https://doi.org/10.5194/amt-6-2403-2013

Lorenz, E., Kühnert, J., Heinemann, D., Nielsen, K. P., Remund, J., & Müller, S. C. (2016). Comparison of global horizontal irradiance forecasts based on numerical weather prediction models with different spatio-temporal resolutions. Progress in Photovoltaics: Research and Applications, 24(12), 1626–1640. https://doi.org/10.1002/pip.2799

Lorenz, E., Nouri, B., Cros, S., Pagh Nielsen, K., Fritz, R., Good, G., Pierro, M., Sanchez Hernandez, G., Lauret, P., David, M., Amaro E Silva, R., Peruchena, C. F., & Cornaro, C. (2024). Forecasting Solar Radiation and Photovoltaic Power. In Best Practices Handbook for the Collection and Use of Solar Resource Data for Solar Energy Applications: Fourth Edition. National Renewable Energy Laboratory. https://doi.org/10.2172/2448063

Mazzola, S., Vergara, C., Astolfi, M., Li, V., Perez-Arriaga, I., & Macchi, E. (2017). Assessing the value of forecast-based dispatch in the operation of off-grid rural microgrids. Renewable Energy, 108, 116–125. https://doi.org/10.1016/j.renene.2017.02.040

Owens, R., & Hewson, T. (2018). ECMWF Forecast User Guide. https://doi.org/10.21957/M1CS7H

Pawel, I. (2014). The Cost of Storage – How to Calculate the Levelized Cost of Stored Energy (LCOE) and Applications to Renewable Energy Generation. Energy Procedia, 46, 68–77. https://doi.org/10.1016/j.egypro.2014.01.159

Perez, R., Ineichen, P., Seals, R., Michalsky, J., & Stewart, R. (1990). Modeling daylight availability and irradiance components from direct and global irradiance. Solar Energy, 44(5), 271–289. https://doi.org/10.1016/0038-092X(90)90055-H

Ramahatana, F., Le Gal La Salle, J., Lauret, P., & David, M. (2022). A more efficient microgrid operation through the integration of probabilistic solar forecasts. Sustainable Energy, Grids and Networks, 100783. https://doi.org/10.1016/j.segan.2022.100783

Randrianantenaina, T. A., Le Gal La Salle, J., Spataru, S. V., & David, M. (2025). Increasing the self-sufficiency of a university campus by expanding the PV capacity while minimizing the energy cost. EPJ Photovoltaics, 16, 7. https://doi.org/10.1051/epjpv/2024048

Ridley, B., Boland, J., & Lauret, P. (2010). Modelling of diffuse solar fraction with multiple predictors. Renewable Energy, 35(2), 478–483. https://doi.org/10.1016/j.renene.2009.07.018

Short, W., Packey, D. J., & Holt, T. (2005). A manual for the economic evaluation of energy efficiency and renewable energy technologies (Repr. from the 1995 ed). University Press of the Pacific.

Straub, N., Herzberg, W., Dittmann, A., & Lorenz, E. (2024). Blending of a novel all sky imager model with persistence and a satellite based model for high-resolution irradiance nowcasting. Solar Energy, 269, 112319. https://doi.org/10.1016/j.solener.2024.112319

Yang, D., Alessandrini, S., Antonanzas, J., Antonanzas-Torres, F., Badescu, V., Beyer, H. G., Blaga, R., Boland, J., Bright, J. M., Coimbra, C. F. M., David, M., Frimane, Â., Gueymard, C. A., Hong, T., Kay, M. J., Killinger, S., Kleissl, J., Lauret, P., Lorenz, E., … Zhang, J. (2020). Verification of deterministic solar forecasts. Solar Energy, 210(20–37), S0038092X20303947. https://doi.org/10.1016/j.solener.2020.04.019